RSC Advances

PAPER

View Article Online
View Journal | View Issue

Cite this: *RSC Adv.*, 2017, **7**, 15851

Reversal aggregation-induced circular dichroism from axial chirality transfer *via* self-assembled helical nanowires†

Fandian Meng, Yuan Sheng, Fei Li, Chengjian Zhu, Yiwu Quan* and Yixiang Cheng*

Received 17th January 2017
Accepted 6th March 2017

DOI: 10.1039/c7ra00703e

rsc.li/rsc-advances

Two chiral binaphthyl-based enantiomers, (*R*/*S*)-**7**, were designed and synthesized by Sonogashira cross-coupling reaction of AIE-active TPE and *O*-BOPHY. Interestingly, the resulting (*R*/*S*)-**7** can exhibit emission enlargement response in DCM/hexane mixtures due to AIE behavior, but fluorescence quenching in THF/H_2O mixtures due to ACQ effect. (*R*/*S*)-**7** can produce gradual reversal AICD (aggregation-induced circular dichroism) signals from solution to aggregation, which can be attributed to axial chirality transfer to self-assembled helical nanowires in aggregation state.

1. Introduction

In the past ten years, fluorine–boron hybrid complexes have attracted much attention on the organic functional materials for optoelectronic devices, solar cell, OLED and bioprobes.[1] It is well known that bis(difluoroboron)-1,2-bis{(1*H*-pyrrol-2-2-yl) methylene}hydrazine (BOPHY) and 4,4-difluoro-4-bora-3*a*,4*a*-diaza-sindacene (BODIPY) dyes have been regarded as excellent chromophores due to their high quantum yields, sharp fluorescent emission band and narrow absorption.[2] However, BOPHY and BODIPY dyes often show small Stokes' shift which often causes serious self-reabsorption affecting the optical properties.[3] It is of great significance to design D–π–A type molecules and prevent the self-reabsorption *via* intramolecular energy transfer (IET) mechanism.[4] Recently, our group reported mirror-image red-color circularly polarized luminescence (CPL) material of chiral BINOL-based *O*-BODIPY enantiomers *via* IET mechanism from the AIE-active tetraphenyl ethylene (TPE) moiety to the chiral *O*-BODIPY chromophore in DCM/hexane mixtures.[5]

Most organic molecules have aggregation-caused quenching (ACQ) effect which is a harmful photophysical effect on their practical applications.[6] Since 2001, Tang's group first found a kind of the propeller-shaped silole molecule with aggregation-induced emission (AIE) feature which could successfully solve the problem of ACQ.[7] Meanwhile, Park and his co-workers also observed a kind of fluorescent organic nanoparticles with aggregation-induced emission enhance (AIEE) response behavior in 2002.[8] Recently, more and more works have been focused on the AIE or AIEE-based functional molecules as optoelectronic devices and biosensors.[9] Therefore developing tunable aggregation-induced CPL (AICPL) materials based on chiral AIE luminogens have received considerable interest in the aggregate state by choosing various chiral unit and chromophores. But so far there have been only a few reports on AICPL materials based on chiral AIE-active organic fluorescence molecules. Especially, it is quite difficult to adjust and control the CPL signal polarization direction of common chiral organic fluorescence molecules without changing chiral configuration.[10] Our group reported reversal AICPL signals of chiral binaphthyl-based molecules from *cis*-conformation in solution to *trans*-conformation in aggregation state due to the dihedral angle enlargement of two naphthyl rings.[11]

Chiral BINOL-based fluorescence molecules have been successfully used for CPL materials due to high chiral induction feature. Moya's group reported a novel CPL material based on chirality perturbing from BINOL moiety to the achiral chromophore (BODIPY).[12] So far, there has been no report on reversal CPL signal from solution system to aggregation state *via* self-assembled helical nanofibers. In this work, we synthesized two chiral binaphthyl-based enantiomers incorporating BODPHY as chromophore and TPE as AIE-active group, which can exhibit AIEE effect in DCM/hexane solution and ACQ effect in THF/H_2O solution, but no change for reverse AICPL signals can be observed in different solution system. Interestingly, reversal AICD signals was observed in THF/H_2O solutions as the increases of water fraction, which can be attributed to the formation of self-assembled helical nanowires in the aggregation state *via* axial chirality transfer.[10a,13] Compared with the previous reports on AIE-active TPE-based molecules, almost all of them showed aggregation-induced emission enhancement (AIEE) response behaviors.[9a,14]

Key Lab of Mesoscopic Chemistry of MOE, Collaborative Innovation Center of Chemistry for Life Sciences, School of Chemistry and Chemical Engineering, Nanjing University, Nanjing 210093, China. E-mail: yxcheng@nju.edu.cn; quanyiwu@nju.edu.cn

† Electronic supplementary information (ESI) available. See DOI: 10.1039/c7ra00703e

2. Results and discussion

The detailed synthesis procedures of (*R*/*S*)-7 can be obtained by the starting product 2,4-dimethyl-1*H*-pyrrole *via* 6 steps in the total yield of 12.3% as shown in Scheme 1. Bis(difluoroboron)-1,2-bis{(1*H*-pyrrol-2-2-yl)methylene}hydrazine (BOPHY) **3**, **4** and **6** were synthesized according to the reported works.[10d,12,15] (*R*/*S*)-**5** was synthesized from **4** and (*R*/*S*)-**BINOL**, and (*R*/*S*)-7 was obtained by palladium-catalyzed Sonogashira coupling reaction of (*R*/*S*)-**5** with **6** in about 64% yield (ESI 2†). Herein, the designed chiral binaphthyl-based *O*-BOPHY enantiomers are composed of three functional moieties: (i) TPE as AIE-active group and energy transfer part; (ii) BINOL as the chiral source; (iii) BOPHY as the acting chromophore.

The UV-vis absorption of (*R*/*S*)-7 was carried out in different solution systems of DCM/hexane and THF/H_2O mixtures as shown in Fig. 1. (*R*/*S*)-7 enantiomers show the similar absorption spectra in both DCM/hexane and THF/H_2O solutions and have three main absorption peaks centered at 230, 336 and 500 nm, which can be regarded as the absorption peaks of the binaphthyl, TPE and BOPHY of three functional moieties, respectively. The UV-vis spectra of (*R*/*S*)-7 did not show obvious change in DCM/hexane mixtures (Fig. 1a), but there appears a little red-shift for TPE (about 6 nm) and BOPHY (about 16 nm) moieties in THF/H_2O mixtures as the increase of the water fraction (Fig. 1b).

In this paper the fluorescence spectra (*R*/*S*)-7 were excited by using 366 nm to avoid self-absorption interference due to the small Stokes' shift of BOPHY chromophore. As is evident from Fig. 2, it can be clearly observed that (*R*/*S*)-7 displays fluorescence emission band at 539 nm with 0.11 of Φ_F (fluorescence quantum yield) in DCM solution (Fig. 2a). Upon the addition of the poor solvent hexane, the emissive intensity of (*R*/*S*)-7 gradually enhances with 5 nm blue-shift at 95% hexane fraction, the Φ_F value can reach as high as 0.31 and 2.94-fold higher than that in DCM solution. Meanwhile, (*R*/*S*)-7 in THF solution has similar fluorescence emission at 538 nm with 0.07 of Φ_F. Interestingly, (*R*/*S*)-7 shows obvious fluorescence quenching response as the increase of water fraction (Fig. 2b), and almost no fluorescence emission signal could be observed at $f_w = 95\%$, which can be regarded as ACQ effect. Based on the results of the dynamic light scattering (DLS) measurement (ESI Fig. S1†), we found the particle size of (*R*/*S*)-7 in THF/water mixtures enlarged from 64.64 nm at $f_w = 60\%$ to 556.33 nm at $f_w = 95\%$, indicating that (*R*/*S*)-7 aggregates produce the solid precipitate in high water fraction.

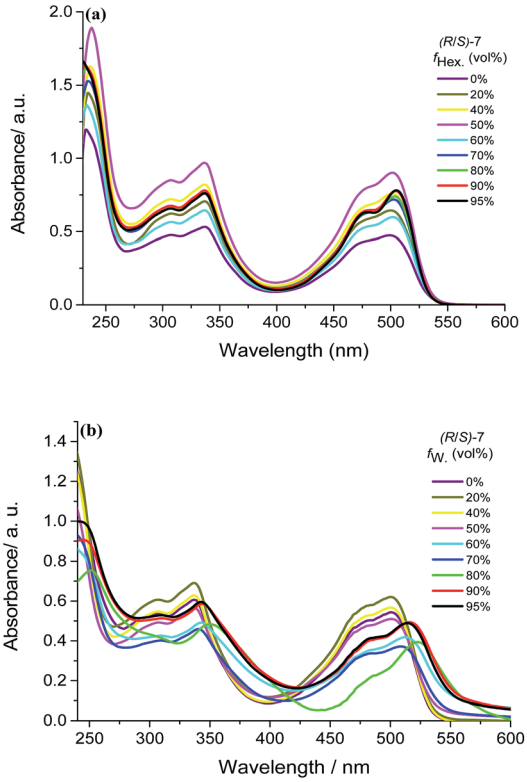

Fig. 1 (a) UV-vis absorption spectra of (*R*/*S*)-7 in DCM/hexane; (b) UV-vis absorption spectra of (*R*/*S*)-7 in THF/H_2O (1.0×10^{-5} mol L^{-1}). f_{HEX} is the volume fraction of hexane, f_w is the volume fraction of water.

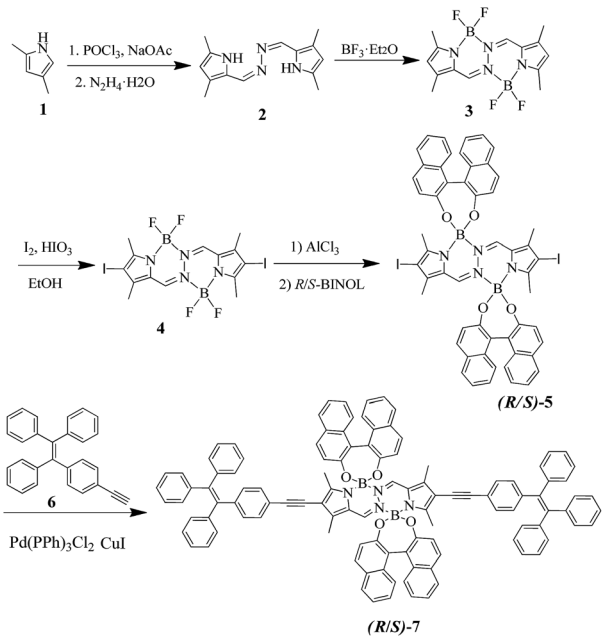

Scheme 1 Synthesis of (*R*/*S*)-7 enantiomers.

On the contrary, (*R*/*S*)-7 can still keep the stable nanoaggregates with a mean diameter of 9.05 nm at 95% in DCM/hexane solution system. Therefore, the morphologies of aggregates in THF/water mixtures were performed by using with scanning electron microscope (SEM). When the fraction of the water is below 70%, (*S*)-7 forms nanorods (Fig. 3, upper). We are very pleased to find that (*S*)-7 can self-assemble to left-handed helical nanowires with length up to micrometers at 5 vol% f_w (Fig. 3, lower).

Herein, we further studied the circular dichroism (CD) spectra to investigate the chirality change feature of (*R*/*S*)-7 from solution to nanoaggregate. The enantiomeric (*R*)-7 and (*S*)-7 can exhibit excellent mirror CD signals in DCM and THF solution (Fig. 4), respectively. Similar to the UV-vis spectra, the CD spectra have

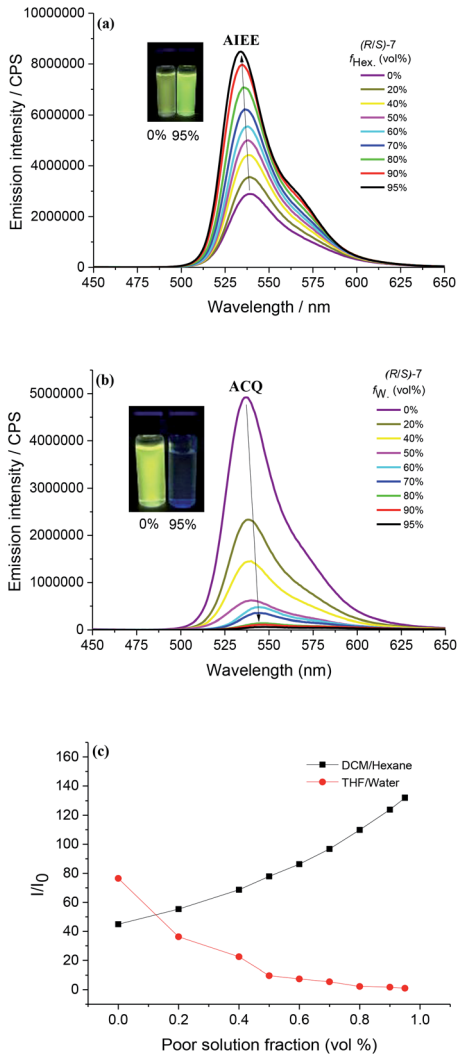

Fig. 2 (a) Fluorescence spectra of (*R*/*S*)-**7** in DCM/hexane; (b) fluorescence spectra of (*R*/*S*)-**7** in THF/H_2O; (c) plot of (I/I_0) values *versus* the compositions of the poor solvent fractions (1.0×10^{-5} mol L^{-1}).

three main absorption signals-about 240 nm for binaphthyl unit, about 340 nm for TPE unit and about 500 nm for BOPHY unit, which indicates that the chirality of binaphthyl unit can effectively transfer to the AIE-active group (TPE) and chromophore moiety (BOPHY). In DCM/hexane mixtures, only the intensity of CD signals at 537 nm from the CD absorption of BOPHY unit shows the gradual decrease as the increase of hexane fraction (Fig. 4a). The g_{abs} compound (*R*)-**7** declined from 7.4×10^{-4} to 3.1×10^{-4}, when the fraction of poor solution increases from 0% to 95%. For THF/water solution, almost no change in CD absorption spectra of (*R*/*S*)-**7** can be observed before 60% water fraction. Interestingly, aggregation-induced CD signals of (*R*/*S*)-**7** exhibit great difference from the Cotton effect peak of BOPHY unit situated at about 490 nm. As the increase of water fraction to 95%, AICD signals appear reversal and redshift to 520 nm (Fig. 4b and c), which may be attributed to axial chirality transfer to self-assembled helical nanowires in aggregation state (Fig. 3).[12] Most importantly, the g_{abs} of (*R*)-**7** also shows reverse change

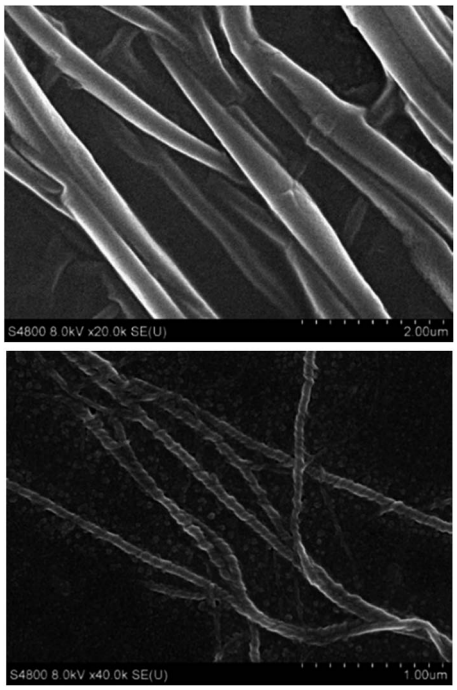

Fig. 3 SEM images of (*S*)-**7** obtained from THF/water (40/60, upper, 5/95, lower, v/v).

from 4.0×10^{-4} to -4.1×10^{-4} while the fraction of poor solution increases from 0% to 95% (Fig. 4b and c).

The interesting AICD response behaviour for (*R*/*S*)-**7** in the maximal absorption band demonstrates that the chirality of binaphthyl moiety can induce the BOPHY chromophore in its ground state, which inspired us to further investigate their CPL property. As is evident from Fig. 5, (*R*/*S*)-**7** can show mirror-image CPL signals centered at about 550 nm from BOPHY chromophore in both DCM and THF solution. Upon addition of poor solvent, almost no change can be observed for the CPL spectra of (*R*/*S*)-**7** in DCM/hexane mixtures, which is similar to CD spectra. But while the fraction of hexane exceeds 90%, CPL signals the *g*-values (g_{lum}) of (*R*/*S*)-**7** have a slight decrease from 5.4×10^{-4} to 2.7×10^{-4}. For THF/H_2O solution system, we found the g_{lum} of (*R*/*S*)-**7** can reach as high as 5.5×10^{-4} and show no obvious change when the water fraction is below 40%. On the contrary, the CPL signal of (*R*/*S*)-**7** almost disappears after the water fraction is over 60%, which is also similar to fluorescence quenching behaviour (ACQ effect). The reason may be attributed to the formation of the solid precipitate at high water fraction, which leads to very weak fluorescence emission (Fig. 2b). In our previous report, chiral BINOL-based *O*-BODIPY enantiomers incorporating TPE as AIE-active group also showed on change on the chiroptical properties of CD and CPL either in DCM solution system or aggregate state in DCM/hexane.[5]

3. Experimental section

Materials and measurements

All reagents and solvents were purchased from commercial sources and analytical grade reagent. NMR spectra were

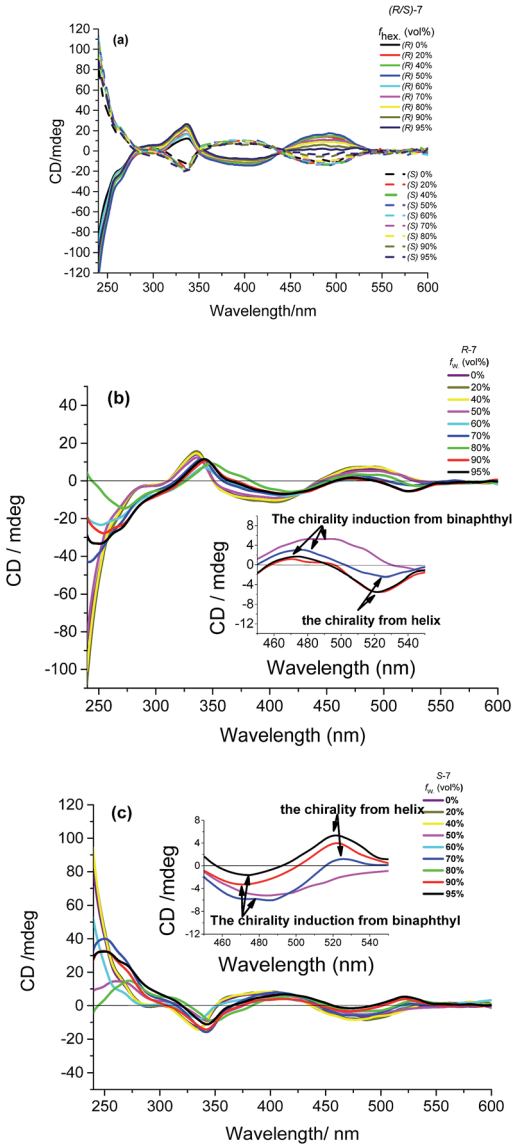

Fig. 4 CD spectra of (*R*/*S*)-**7**: (a) in DCM/hexane mixtures; (b) and (c) in THF/H_2O mixtures (1.0×10^{-5} mol L^{-1}).

recorded on Bruker Avance 400 spectrometer, using TMS as an internal standard. Fluorescence spectra recorded with an RF-5301PC spectrometer. UV-vis spectra and circular dichroism (CD) were obtained on JASCO J-810 spectropolarimeter. Circularly polarized luminescence (CPL) spectra were acquired using the JASCO CPL-200 spectrofluoropolarimeter. Elemental analysis was performed on an Elementar Vario MICRO analyzer. All optical measurements were investigated in THF and THF/water mixtures with a uniform concentration (1.0×10^{-5} mol L^{-1}). The level of CPL properties is evaluated by the luminescence dissymmetry factor (g_{lum}), which is calculated as $g_{lum} = 2(I_L - I_R)/(I_L + I_R) = 2\Delta I/I$, where I_L and IR represent the emission intensities of left and right circularly polarized luminescence, respectively. Experimentally, the value of glum is calculated by $\Delta I/I$ = [ellipticity/(32 980/ln 10)]/(unpolarized PL intensity) at the CPL extremum.

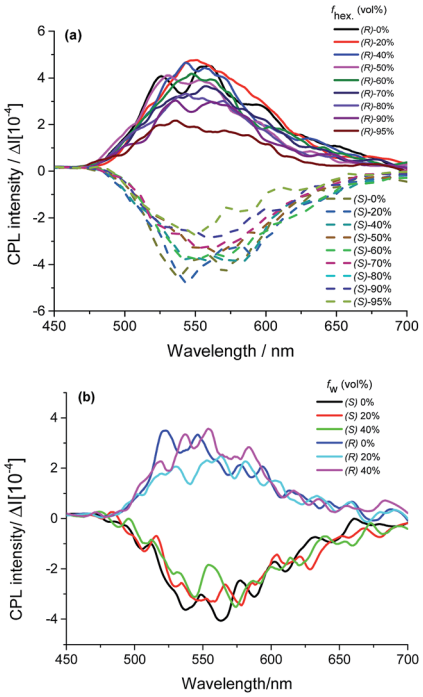

Fig. 5 CPL spectra of (*R*)-**7** and (*S*)-**7** in DCM/hexane mixtures (a) and THF/H_2O mixtures (b) (1.0×10^{-5} mol L^{-1}).

Quantum yields were determined by the optically dilute relative method using the following equation: $\Phi_S = \Phi_R \times [(I_S \times A_R)/(I_R \times A_S)][(n_S)^2/(n_R)^2]$ where Φ_S is the quantum yield of the lanthanide complex, Φ_R is the quantum yield of the reference, A is the absorbance at the excitation wavelength, I is the relative intensity of the excitation light at the same wavelength, n is the refractive index, and the subscripts "S" and "R" refer to sample and reference, respectively. In this case, quinine sulfate in 0.5 M sulfuric acid was used as reference ($\Phi_R = 0.55$).

Synthesis of (*R*/*S*)-5

A mixture of **4** (464 mg, 1 mmol), and aluminum chloride (633 mg, 4 mmol) in dry CH_2Cl_2 (20 mL), was reflux until reaction completion (reaction monitoring by TLC), then, a solution of the corresponding enantiopure 1,1′-bi(2-naphthol) ((1*R*)-BINOL or (1*S*)-BINOL, 858 mg, 3 mmol) in anhydrous acetonitrile (10 mL) was added dropwise. The resulting mixture was stirred at room temperature for additional 6 h, washed with brine (1×10 mL) and dried over anhydrous Na_2SO_4. After filtration and solvent evaporation under reduced pressure, the obtained residue was purified by flash chromatography (petroleum ether) to afford **5** as an orange solid (318 mg, 35%). ^{1}H NMR (300 MHz, $CDCl_3$): δ 8.84 (m, 4H), 8.04 (m, 4H), 7.79–7.44 (m, 14H), 7.04 (m, 4H), 2.14 (s, 6H), 2.04 (s, 6H).

Synthesis of (*R*/*S*)-7

A mixture of compound (*R*/*S*)-**5** (200 mg, 0.18 mmol), **6** (138.33 mg, 0.39 mmol), $Pd(PPh_3)_2Cl_2$ (5% mmol), CuI (5% mmol) were added to THF (20 mL) and Et_3N (10 mL) under nitrogen atmosphere. The reaction mixture was stirred at 80 °C

for 36 h. After cooling to room temperature, the solvent was removed under reduced pressure. The residue was purified by column chromatography deactivated basic alumina (petroleum ether/dichloromethane, 4/1) to afford (*R*/*S*)-7 as a red solid.

(*R*)-7: (176 mg, 62.1%) ^{1}H NMR (300 MHz, $CDCl_3$) δ 7.93 (m, 6H), 7.84 (d, J = 8.1 Hz, 2H), 7.73 (d, J = 8.8 Hz, 2H), 7.49 (d, J = 8.7 Hz, 2H), 7.36 (m, 8H), 7.21–6.94 (m, 42H), 6.88 (d, J = 8.7 Hz, 2H), 1.92 (s, 6H), 1.64 (s, 6H). ^{13}C NMR (75 MHz), δ 154.10, 153.14, 152.53, 143.72, 143.43, 143.38, 143.27, 141.54, 141.16, 140.14, 136.09, 133.47, 133.01, 131.31, 131.26, 131.24, 130.54, 130.22, 130.19, 129.93, 129.78, 128.14, 128.00, 127.78, 127.68, 127.61, 127.21, 126.61, 126.55, 126.53, 125.90, 125.57, 124.11, 123.73, 122.69, 122.59, 122.20, 121.96, 121.85, 121.03, 112.92, 95.37, 81.59, 29.67, 29.63, 13.21, 9.85. Anal. calcd for $C_{110}H_{76}B_2N_4O_4$: C, 85.82; H, 4.98. Found: C, 85.80; H, 5.02. MS (ESI, m/z): 1539.76 $[M + H]^+$.

(*S*)-7: (182 mg, 64.2%) anal. calcd for $C_{110}H_{76}B_2N_4O_4$: C, 85.82; H, 4.98. Found: C, 85.79; H, 4.99. MS (ESI, m/z): 1539.76 $[M + H]^+$.

4. Conclusion

In summary, the chiral BOPHY-based enantiomers incorporating TPE group can exhibit emission enlargement response in DCM/hexane due to AIE behavior, but fluorescence quenching in THF/H_2O due to ACQ effect. Reversal AICD signals can be observed from solution to aggregation only in THF/H_2O due to axial chirality transfer to self-assembled helical nanowires in aggregation state. The mirror-image CPL signals can be detected in DCM/hexane and low water fraction of THF/H_2O.

Acknowledgements

We would like to thank Prof. Zhiyong Tang at NCNST for their kind help on CPL measurement. This work was supported by the National Natural Science Foundation of China (21474048, 21674046, 51673093).

Notes and references

1 (*a*) X. Wang, H. Liu, J. Cui, Y. Wu, H. Lu, J. Lu, Z. Liu and W. He, *New J. Chem.*, 2014, **38**, 1277; (*b*) R. S. Singh, M. Yadav, R. K. Gupta, R. Pandey and D. S. Pandey, *Dalton Trans.*, 2013, **42**, 1696; (*c*) S. Guieu, F. Cardona, J. Rocha and A. M. S. Silva, *New J. Chem.*, 2014, **38**, 5411; (*d*) A. Haefele, C. Zedde, P. Retailleau, G. Ulrich and R. Ziessel, *Org. Lett.*, 2010, **12**, 1672; (*e*) Y. Kubota, Y. Sakuma, K. Funabiki and M. Matsui, *J. Phys. Chem. A*, 2014, **118**, 8717.

2 (*a*) Q. Huaulmé, A. Mirloup, P. Retailleau and R. Ziessel, *Org. Lett.*, 2015, **17**, 2246; (*b*) A. Mirloup, Q. Huaulmé, N. Leclerc, P. Lévêque, T. Heiser, P. Retailleaud and R. Ziessel, *Chem. Commun.*, 2015, **51**, 14742; (*c*) I. S. Tamgho, A. Hasheminasab, J. T. Engle, V. N. Nemykin and C. J. Ziegler, *J. Am. Chem. Soc.*, 2014, **136**, 5623; (*d*) H. M. Rhoda, K. Chanawanno, A. J. King, Y. V. Zatsikha, C. J. Ziegler and V. N. Nemykin, *Chem.–Eur. J.*, 2015, **21**, 18043.

3 (*a*) A. Brzeczek, K. Piwowar, W. Domagala, M. M. Mikołajczyk, K. Walczakb and P. Wagner, *RSC Adv.*, 2016, **6**, 36500; (*b*) J. Liao, Y. Xu, H. Zhao, Y. Wang, W. Zhang, F. Peng, S. Xie and X. Yang, *RSC Adv.*, 2015, **5**, 86453; (*c*) A. M. Courtis, S. A. Santos, Y. Guan, J. A. Hendricks, B. Ghosh, D. M. Szantai-Kis, S. A. Reis, J. V. Shah and R. Mazitschek, *Bioconjugate Chem.*, 2014, **25**, 1043; (*d*) J. Liao, Y. Wang, Y. Xu, H. Zhao, X. Xiao and X. Yang, *Tetrahedron*, 2015, **71**, 5078.

4 (*a*) B. Cosut, *Dyes Pigm.*, 2014, **100**, 11; (*b*) L. Kong, H. L. Wong, A. Y. Y. Tam, W. H. Lam, L. Wu and V. W. W. Yam, *ACS Appl. Mater. Interfaces*, 2014, **6**, 1550; (*c*) M. Klaper and T. Linker, *J. Am. Chem. Soc.*, 2015, **137**, 13744; (*d*) C. Sohn, J. Jeong, J. H. Lee, B. H. Choi, H. Hwang, G. T. Bae, K. M. Lee and M. H. Park, *Dalton Trans.*, 2016, **45**, 5825; (*e*) E. Sen, K. Meral and S. Atılgan, *Chem.–Eur. J.*, 2016, **22**, 736; (*f*) M. J. Leonardi, M. R. Topka and P. H. Dinolfo, *Inorg. Chem.*, 2012, **51**, 13114; (*g*) F. Sozmen, B. S. Oksal, O. A. Bozdemir, O. Buyukcakir and E. U. Akkaya, *Org. Lett.*, 2012, **14**, 5286.

5 (*a*) M. Baglan, S. Ozturk, B. Gür, K. Meral, U. Bozkaya, O. A. Bozdemir and S. Atlgan, *RSC Adv.*, 2013, **3**, 15866; (*b*) S. Guo, L. Ma, J. Zhao, B. Küçüköz, A. Karatay, M. Hayvali, H. G. Yaglioglu and A. Elmali, *Chem. Sci.*, 2014, **5**, 489; (*c*) A. Harriman, G. Izzet and R. Ziesse, *J. Am. Chem. Soc.*, 2006, **128**, 10868.

6 (*a*) X. Ma, R. Sun, J. Cheng, J. Liu, F. Gou, H. Xiang and X. Zhou, *J. Chem. Educ.*, 2016, **93**, 345; (*b*) M. Yang, D. Xu, W. Xi, L. Wang, J. Zheng, J. Huang, J. Zhang, H. Zhou, J. Wu and Y. Tian, *J. Org. Chem.*, 2013, **78**, 10344.

7 J. Luo, Z. Xie, J. W. Y. Lam, L. Cheng, H. Chen, C. Qiu, H. S. Kwok, X. Zhan, Y. Liu, D. Zhu and B. Z. Tang, *Chem. Commun.*, 2001, 1740.

8 B. K. An, S. K. Kwon, S. D. Jung and S. Y. Park, *J. Am. Chem. Soc.*, 2002, **124**, 14410.

9 (*a*) J. Mei, N. L. C. Leung, R. T. K. Kwok, J. W. Y. Lam and B. Z. Tang, *Chem. Rev.*, 2015, **115**, 11718; (*b*) P. Krukowski, T. Tsuzuki, Y. Minagawa, N. Yajima, S. Chaunchaiyakul, M. Akai-Kasaya, A. Saito, Y. Miyake, M. Katayama and Y. Kuwahara, *J. Phys. Chem. C*, 2016, **120**, 3964; (*c*) J. Xiong, W. Xie, J. Sun, J. Wang, Z. Zhu, H. Feng, D. Guo, H. Zhang and Y. Zheng, *J. Org. Chem.*, 2016, **81**, 3720; (*d*) Z. Zhu, J. Qian, X. Zhao, W. Qin, R. Hu, H. Zhang, D. Li, Z. Xu, B. Z. Tang and S. He, *ACS Nano*, 2016, **10**, 588; (*e*) R. Hu, N. L. C. Leung and B. Z. Tang, *Chem. Soc. Rev.*, 2014, **43**, 4494; (*f*) X. Zhang, K. Wang, M. Liu, X. Zhang, L. Tao, Y. Chen and Y. Wei, *Nanoscale*, 2015, **7**, 11486; (*g*) L. Liu, B. Wu, P. Yu, R. Zhuo and S. Huang, *Polym. Chem.*, 2015, **6**, 5185.

10 (*a*) J. Liu, H. Su, L. Meng, Y. Zhao, C. Deng, J. C. Y. Ng, P. Lu, M. Faisal, J. W. Y. Lam, X. Huang, H. Wu, K. S. Wong and B. Z. Tang, *Chem. Sci.*, 2012, **3**, 2737; (*b*) Q. Ye, D. Zhu, H. Zhang, X. Lu and Q. Lu, *J. Mater. Chem. C*, 2015, **3**, 6997; (*c*) R. Tempelaar, A. Stradomska, J. Knoester and F. C. Spano, *J. Phys. Chem. B*, 2011, **115**, 10592; (*d*) S. Zhang, Y. Wang, F. Meng, C. Dai, Y. Cheng and C. Zhu, *Chem. Commun.*, 2015, **51**, 9014; (*e*) T. Ikeda, T. Masuda,

T. Hirao, J. Yuasa, H. Tsumatori, T. Kawai and T. Haino, *Chem. Commun.*, 2012, **48**, 6025; (*f*) J. Kumar, H. Tsumatori, J. Yuasa, T. Kawai and T. Nakashima, *Angew. Chem., Int. Ed.*, 2015, **54**, 5943.

11 Y. Sheng, D. Shen, W. Zhang, H. Zhang, C. Zhu and Y. Cheng, *Chem.–Eur. J.*, 2015, **21**, 13196.

12 E. M. Sánchez-Carnerero, F. Moreno, B. L. Maroto, A. R. Agarrabeitia, M. J. Ortiz, B. G. Vo, G. Muller and S. de la Moya, *J. Am. Chem. Soc.*, 2014, **136**, 3346.

13 (*a*) T. Kaseyama, S. Furumi, X. Zhang, K. Tanaka and M. Takeuchi, *Angew. Chem., Int. Ed.*, 2011, **50**, 3684; (*b*) L. Wang, N. Suzuki, J. Liu, T. Matsuda, N. A. A. Rahim, W. Zhang, M. Fujiki, Z. Zhang, N. Zhou and X. Zhu, *Polym. Chem.*, 2014, **5**, 5920; (*c*) M. Hentschel, V. E. Ferry and A. P. Alivisatos, *ACS Photonics*, 2015, **2**, 1253.

14 (*a*) L. He, L. Li, X. Liu, J. Wang, H. Huang and W. Bu, *Polym. Chem.*, 2016, **7**, 3722; (*b*) X. Du, J. Qi, Z. Zhang, D. Ma and Z. Y. Wang, *Chem. Mater.*, 2012, **24**, 2178; (*c*) S. Mi, J. Wu, J. Liu, Z. Xu, X. Wu, G. Luo, J. Zheng and C. Xu, *ACS Appl. Mater. Interfaces*, 2015, **7**, 27511.

15 (*a*) X. Liu, H. Nan, W. Sun, Q. Zhang, M. Zhan, L. Zou, Z. Xie, X. Li, C. Lu and Y. Cheng, *Dalton Trans.*, 2012, **41**, 10199; (*b*) C. Dai, D. Yang, W. Zhang, B. Bao, Y. Cheng and L. Wang, *Polym. Chem.*, 2015, **6**, 3962; (*c*) C. Yu, L. Jiao, P. Zhang, Z. Feng, C. Cheng, Y. Wei, X. Mu and E. Hao, *Org. Lett.*, 2014, **16**, 3048.